Comparison of mobility extraction methods based on field-effect measurements for graphene

Cite as: AIP Advances **5**, 057136 (2015); https://doi.org/10.1063/1.4921400
Submitted: 25 March 2015 . Accepted: 07 May 2015 . Published Online: 15 May 2015

Hua Zhong, Zhiyong Zhang, Haitao Xu, Chenguang Qiu, and Lian-Mao Peng

Comparison of mobility extraction methods based on field-effect measurements for graphene

Hua Zhong, Zhiyong Zhang,[a] Haitao Xu, Chenguang Qiu, and Lian-Mao Peng[a]

Key Laboratory for the Physics and Chemistry of Nanodevices and Department of Electronics, Peking University, Beijing 100871, China

(Received 25 March 2015; accepted 7 May 2015; published online 15 May 2015)

Carrier mobility extraction methods for graphene based on field-effect measurements are explored and compared according to theoretical analysis and experimental results. A group of graphene devices with different channel lengths were fabricated and measured, and carrier mobility is extracted from those electrical transfer curves using three different methods. Accuracy and applicability of those methods were compared. Transfer length method (TLM) can obtain accurate density dependent mobility and contact resistance at relative high carrier density based on data from a group of devices, and then can act as a standard method to verify other methods. As two of the most popular methods, direct transconductance method (DTM) and fitting method (FTM) can extract mobility easily based on transfer curve of a sole graphene device. DTM offers an underestimated mobility at any carrier density owing to the neglect of contact resistances, and the accuracy can be improved through fabricating field-effect transistors with long channel and good contacts. FTM assumes a constant mobility independent on carrier density, and then can obtain mobility, contact resistance and residual density stimulations through fitting a transfer curve. However, FTM tends to obtain a mobility value near Dirac point and then overestimates carrier mobility of graphene. Comparing with the DTM and FTM, TLM could offer a much more accurate and carrier density dependent mobility, that reflects the complete properties of graphene carrier mobility. [http://dx.doi.org/10.1063/1.4921400]

Graphene has been recognized as a promising material for electronic applications owing to its outstanding electronic properties.[1–3] In the past decade, many methods have been developed by material scientists and engineers to prepare large scale and high-quality graphene samples,[4–9] which provide the base for the device-level applications of graphene,[10] and carrier mobility u is one of the most concerned figure of merits of the graphene quality as they grown. Generally, carrier mobility is extracted through data from two kinds of measurements, *i.e.*, Hall measurements[5,11,12] or field-effect measurements.[4,6,13] Hall measurements present accurate measurement of the carrier mobility, and involve complicate device fabrication process and measurement technique. Thus, field-effect measurements become the most popular means to estimate carrier mobility owing to its simplicity and feasibility. In literature, there are two widely used carrier mobility extraction methods that based on the transfer characteristics from field-effect measurements of graphene. One is the traditional field-effect mobility model, which we called direct transconductance method (DTM), and the other is a constant mobility model proposed by Kim *et al.*,[14] which we named fitting method (FTM). The DTM uses transconductance g_m and gate induced carrier density of the measured device to calculate mobility, with directly ignoring the effect of contact resistance R_c. The FTM takes contact resistance into account and fits the whole transfer curve, and then

[a]Authors to whom correspondence should be addressed. Electronic addresses: zyzhang@pku.edu.cn and lmpeng@pku.edu.cn

carrier mobility, contact resistance and residual carrier density n_0 are all retrieved. The fact that the measured total resistance R_{total} of a graphene field-effect transistor (GFET) includes both channel resistance (co-determined by carrier mobility and density) and contact resistance requires eliminating, or at least minimizing, the effect of contact resistance for accurate carrier mobility extraction. However impacts of the contact resistance on the validity and accuracy of these two popular methods have never been explored for graphene carrier mobility estimation.

In this work, we will develop transfer length method (TLM) to extract the contact resistance and carrier mobility in GFETs under room and liquid nitrogen temperature (300 K and 77 K). Then, the obtained carrier mobility will be treated as a benchmark to inspect the validity and accuracy of these two mentioned popular carrier mobility extraction methods, and effects of the contact resistance will be fully discussed. By comparing the obtained carrier mobility through three different methods, some suggestions and directions for improving accuracy of these two commonly used approximate methods will be presented.

TLM is a standard method to measure the contact resistance of graphene/metal junction,[15] and then can further expanded to extract carrier mobility of graphene, as sheet resistance (conductivity) of graphene layer is also obtained in the TLM.[16] The precondition of TLM is to fabricate a group of uniform graphene devices with different channel lengths and the same channel width. Back-gated GFETs with six different channel lengths, channel length L varies from 1 um to 6 um in a step of 1 um, were fabricated on mechanically exfoliated single layer graphene flake, which locates on a heavily p-doped silicon substrate covered with 285 nm silicon oxide. Single layer property of this graphene flake was confirmed by optical microscope and Raman spectrum. Graphene sample was patterned into a long strip with width of 2.2 um by electron-beam lithography (EBL) and reactive ion etching (RIE). The contact electrode windows were defined through another EBL process, and then Pd/Au (30/50 nm) film was deposited by electron-beam evaporation (EBE). After a standard lift-off process, graphene devices were fabricated. The scanning electron microscopy (SEM) image of the group of GFETs is shown in the inset of Fig. 1(a). Transfer characteristics of these GFETs were measured in vacuum at room temperature (300 K) and liquid nitrogen temperature (77 K) respectively, and presented in Fig. 1(a) and 1(b), where the minimum current points (Dirac voltage points) have been shifted to zero.

The well-developed transfer length method was used to extract contact resistance based on the group of I_{ds}-V_g data, and then carrier mobility can be retrieved through back-gate voltage dependent resistance of graphene channel. Specifically the total resistance R_{total} consists of channel resistance from graphene and contact resistance from graphene/metal junction, and that is

$$R_{total}(L) = R_{sheet}L/W + 2R_c/W. \tag{1}$$

R_{sheet} is the sheet resistance of graphene, and R_c is the contact width (same as the channel width) W normalized contact resistance.

By linear fitting R_{total} of GFETs with different L under the same net gate voltage (V_g-V_{Dirac}), R_{sheet} and R_c at this gate voltage were achieved from the slope and intercept respectively, and then gate voltage dependent R_{sheet} and R_c curves were obtained as shown in Fig. 1(c). Both of R_c and R_{sheet} are dependent on the gate voltage, and also asymmetric with respect to the Dirac point. Asymmetry of R_c arises from the p-type doping Pd contact,[15,17,18] and asymmetry of R_{sheet} is due to the different Coulomb scattering strength to the residual charges between hole and electron.[19,20] The carrier mobility u_{TLM} of graphene was extracted from R_{sheet}-(V_g-V_{Dirac}) relation through

$$\mu_{TLM}\left(V_g - V_{Dirac}\right) = 1/qn\left(V_g - V_{Dirac}\right) R_{sheet}\left(V_g - V_{Dirac}\right), \tag{2}$$

in which n (V_g - V_{Dirac}) is the gate voltage dependent carrier density in graphene. Generally, carrier density n (V_g - V_{Dirac}) contains residual charge density induced by charged impurities and net charge density induced by gate voltage, which was given by the assumption that

$$n(V_g - V_{Dirac}) = \sqrt{n_0^2 + (C_g\left|V_g - V_{Dirac}\right|)^2}, \tag{3}$$

where n_0 is residual charge density, and C_g is the unit back-gate capacitance of GFETs. As these back-gated GFETs were fabricated on Si substrate with certain thickness of thermal grown SiO_2,

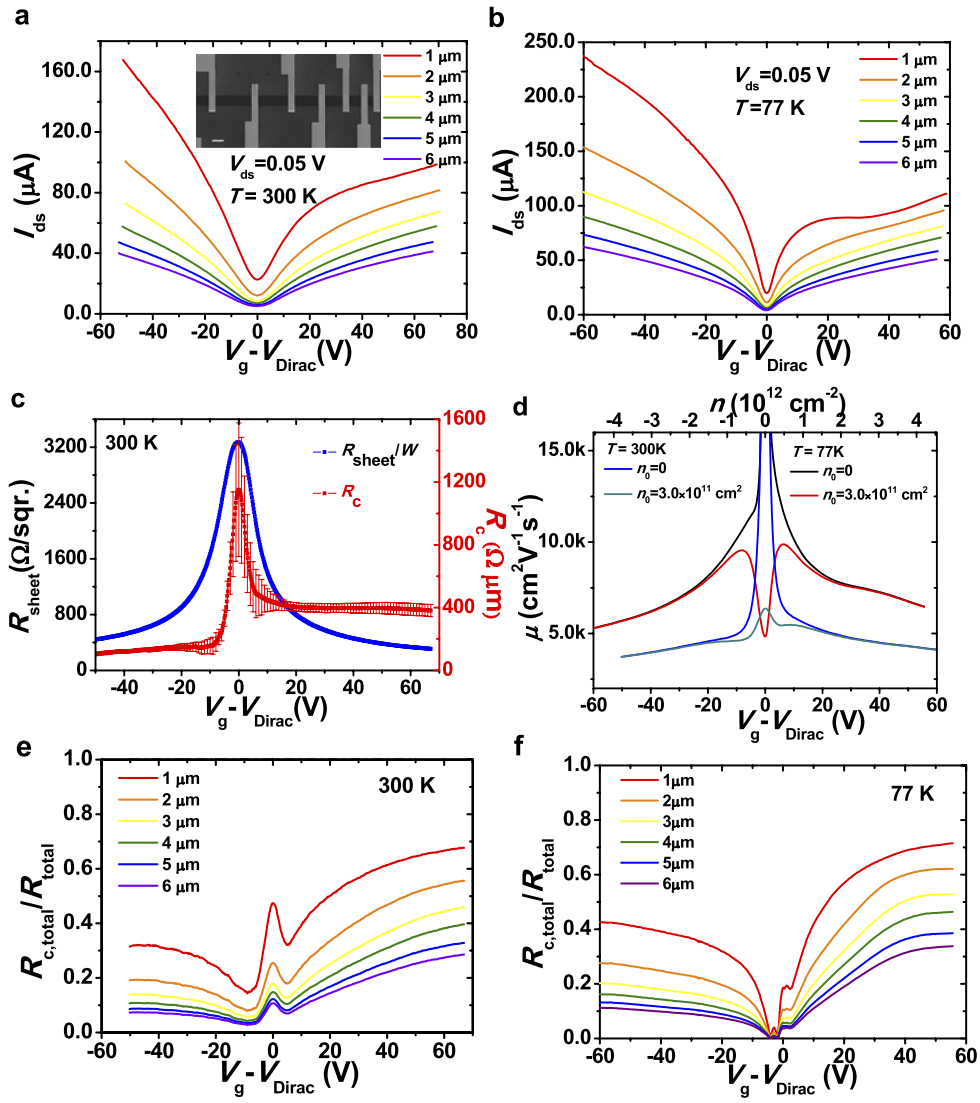

FIG. 1. Carrier mobility extraction and analyses through TLM method. (a) Transfer characteristics of a group of GFETs with different channel length measured at 300 K. Inset: SEM image of the GFETs. The scale bar is 2 um. (b) Transfer characteristics of the same group of GFETs at 77 K. (c) Sheet resistance and contact resistance derivation by TLM as functions of gate voltage. (d) Gate voltage (or carrier density) dependent carrier mobility with assumed residual carrier density 300 K and 77K. Ratio between total contact resistance and total resistance of GFETs (e) at 300 K and (f) at 77 K.

here the thickness of silicon oxide is 285 nm, the back-gate capacitance is exactly the capacitance of the SiO_2 layer, that is

$$C_g = \varepsilon\varepsilon_0/t_{ox}. \tag{4}$$

ε and ε_0 are relative and absolute dielectric constant, t_{ox} is the SiO_2 thickness. Note, quantum capacitance of graphene was neglected since it is much larger than the insulator capacitance.

According to Eq. (2), (3) and (4), the carrier mobility can be extracted based on the R_{sheet} -(V_g-V_{Dirac}) curve in Fig. 1(c) if the residual carrier density n_0 is known. Here, an empirical value of n_0 (3.0×10^{11} cm^{-2}) was employed, which will be found is not that important later. Fig. 1(d) shows the gate voltage (carrier density) dependent carrier mobility, assuming n_0 as 0 and 3.0×10^{11} cm^{-2}, at 300 K and 77 K. As seen, the effect of residual density n_0 on transport behaviour of graphene is only impactive near the Dirac point, and is negligible far away from Dirac point, where the gate induced net carrier density exceeds 2.0×10^{12} cm^{-2}. In fact, the carrier mobility at relative

high carrier density is valuable for practical electronic applications. Therefore carrier mobility at the whole measured region was achieved as shown in Fig. 1(d). It is obviously that the extracted carrier mobility depends on carrier density as traditional semiconductors[16] which is consistent with the published theory and Hall measurements results.[21,22] The extracted carrier mobility also shows a temperature dependence, which is attributed to the scattering of surface polar phonons of SiO_2 substrate.[22–24]

Base on the data from a group of field-effect graphene devices, the TLM method theoretically eliminates the effects of contact resistance, which is important for precise carrier mobility estimation. As shown in Fig. 1(e) and 1(f), gate voltage dependent $R_{c,total}/R_{total}$ curves of the group of G-FETs were plotted respectively at two measured temperatures. $R_{c,total}/R_{total}$ presents the proportion of total contact resistance $R_{c,total}$ $(2R_c/W)$ in the whole channel resistance. Four points can be deduced from Fig. 1(e) and 1(f). Firstly the ratio of $R_{c,total}$ declines with increase of channel length since channel resistance is proportional to the channel length. Secondly the ratio of $R_{c,total}$ strongly depends on the gate voltage and increases with gate voltage at large gate bias, which could exceed 1/2 for short channel device. It should be noted that there are two minimum values of $R_{c,total}/R_{total}$ located at n-branch and p-branch respectively, where impacts of contact resistance is minimum. Thirdly the $R_{c,total}/R_{total}$ in n-branch is obviously larger than that in p-branch owing to the asymmetry of contact resistance induced by Pd contacts. As shown in Fig. 1(c), R_c in n-branch is around 400 Ω um, while it is about 100 Ω um in p-branch. Lastly the$R_{c,total}/R_{total}$ ratio is also affected by temperature, that the ratio under 77 K is obviously larger than that under 300 K owing to the increased carrier mobility (Fig. 1(d)) and almost constant contact resistance.[25] So, the validity and accuracy of mobility extraction methods strongly depends on how to deal with the contact resistance.

In the direct transconductance method (DTM), mobility is extract according to the gate voltage dependent transconductance, *i.e.* through

$$\mu_{DTM} = g_m \frac{L}{W V_{ds} C_g}, \tag{5}$$

where $g_m = \partial I_{ds}/\partial V_g$ is transconductance and the mobility u_{DTM} is the field-effect mobility. In Fig. 2(a), the field-effect mobility of six GFETs at 300 K were plotted, and the mobility extracted by TLM was also presented as a real mobility for comparison. Due to the ignorance of contact resistance, field-effect mobility is always lower than the real mobility at any given gate voltage, and the gap between field-effect mobility and actual value depends on gate voltage, channel length and conduction type. Besides, three other points can also be concluded from Fig. 2(a). (1) The difference declines with increasing channel length, which means the accuracy of DTM mobility is higher in longer channel device. (2) The difference in p-branch is much smaller than that in n-branch, which implies lower contact resistance provides higher accuracy, as the ratio of $R_{c,total}/R_{total}$ in n-branch is larger. (3) The difference depends on the gate voltage, and reaches a minimum value at a certain V_g, which is close to the peak transconductance point, and then the DTM mobility is closest to the real mobility. In Fig. 2(c), the DTM mobility and ratio of $R_{c,total}/R_{total}$ of a 6-*u*m long GFET were plotted together, the relation between maximum DTM u_{DTM} and minimum $R_{c,total}/R_{total}$ is quite clear. Therefor to achieve high and accurate field-effect mobility, impacts of contact resistance should be minimized, and thus, good contact should be formed or long channel should be fabricated.

In fact, peak field-effect mobility is usually considered as the mobility of GFETs, since it is highest possible mobility that can be achieved from the DTM. Fig. 2(e) shows the DTM peak mobility of GFETs with different channel lengths. Obviously, the DTM peak mobility of longer GFETs are closer to its real value than that of shorter device. And in the same GFET, hole mobility is more accurate than electron mobility since the $R_{c,total}/R_{total}$ is much larger in n-branch than that in p-branch. As a comparison we also extracted and analysis the carrier mobility of the same group of GFETs at 77 K based on DTM as shown in Fig. 2(b), 2(d) and 2(f). As the contact resistance of GFETs almost remains unchanged and channel resistance decreased due to the carrier mobility increase, $R_{c,total}/R_{total}$ at 77 K is larger than at 300 K as shown in Fig. 2(d), and the accuracy of DTM peak mobility thus becomes worse as shown in Fig. 2(f).

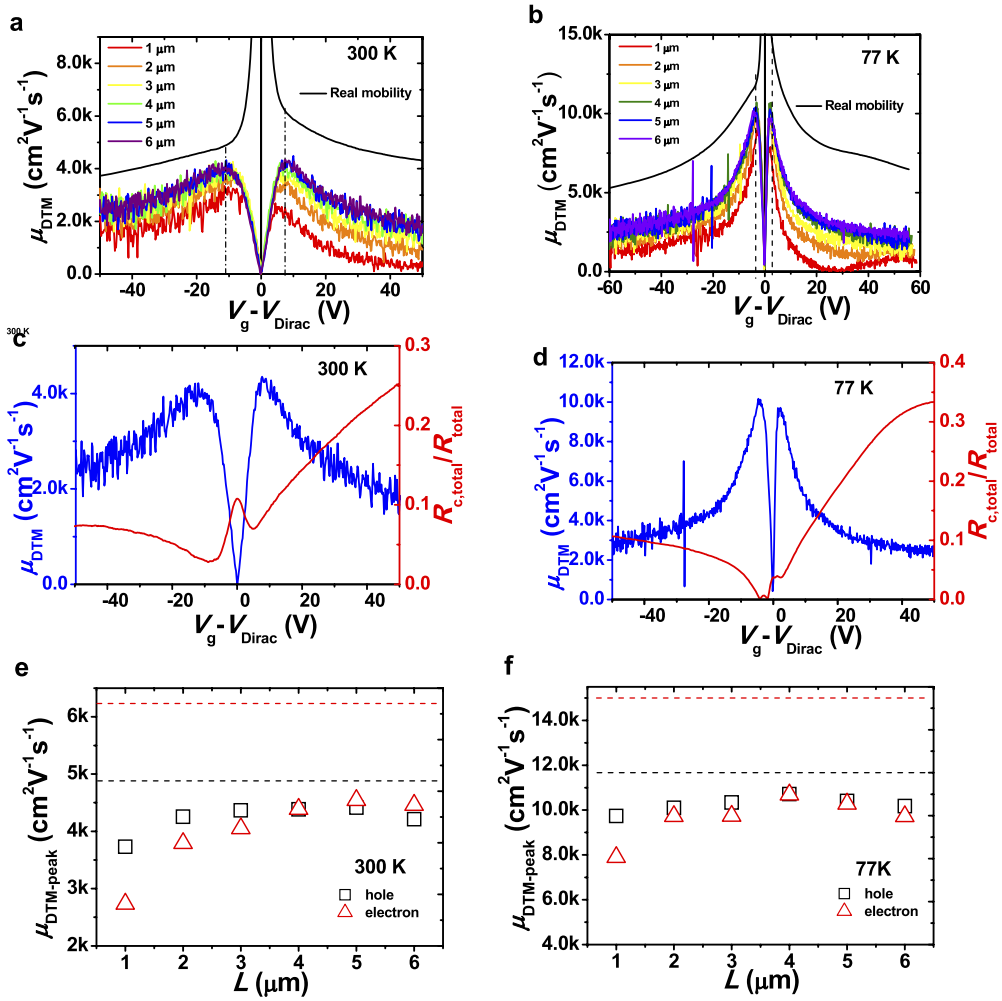

FIG. 2. Direct transconductance method for mobility extraction. (a) V_g dependent field-effect mobility of six GFETs at 300 K. The black curve represents the real mobility retrieved through TLM method with n_0 =0. (b) V_g dependent field-effect mobility of six GFETs at 77 K. The black curve also represents the real mobility retrieved through TLM method. (c) V_g dependent field-effect mobility and $R_{c,total}/R_{total}$ of the GFET with $L = 6$ um at 300 K. (d) V_g dependent field-effect mobility and $R_{c,total}/R_{total}$ of the GFET with $L = 6$ um at 77 K. (e) Hole and electron peak field-effect mobility as a function of channel length at 300 K. The black and red dotted lines represent hole and electron mobility at V_g of peak transconductance (in Fig. 2(a)) by TLM method. (f) Hole and electron peak field-effect mobility as a function of channel length at 77 K. The black and red dotted lines represent hole and electron mobility at V_g of peak transconductance (in Fig. 2(b)) by TLM method.

Another popular method for mobility extraction in graphene is the fitting method (FTM) developed by Kim *et al.* in 2009,[14] which is also based on the transfer curves of a sole GFET. The total resistance of a GFET was given by

$$R_{\text{total}} = R_c + \frac{L}{W}\frac{1}{u_{\text{FTM}} n (V_g - V_{\text{Dirac}})}, \tag{6}$$

where n is the gate dependent carrier mobility given by Eq. (3) with quantum capacitance ignored, and the carrier mobility u_{FTM} and contact resistance R_c in Eq. (6) were assumed to be constant. Fit of the transfer curve through Eq. (6), parameters as carrier mobility, contact resistance and residual carrier density for both of the n-branch and the p-branch can be obtained. As typical examples, transfer curves of the GFET with L = 6 um at 300 K and 77 K were fitted as shown in Fig. 3(a) and 3(b) respectively. At 300 K, the fitted mobility are 4472 cm^2 V^{-1} s^{-1} for hole and 5591 cm^2 V^{-1} s^{-1} for electron, and the contact resistance in the p-branch and n-branch are 264 Ω um and 665 Ω um. On

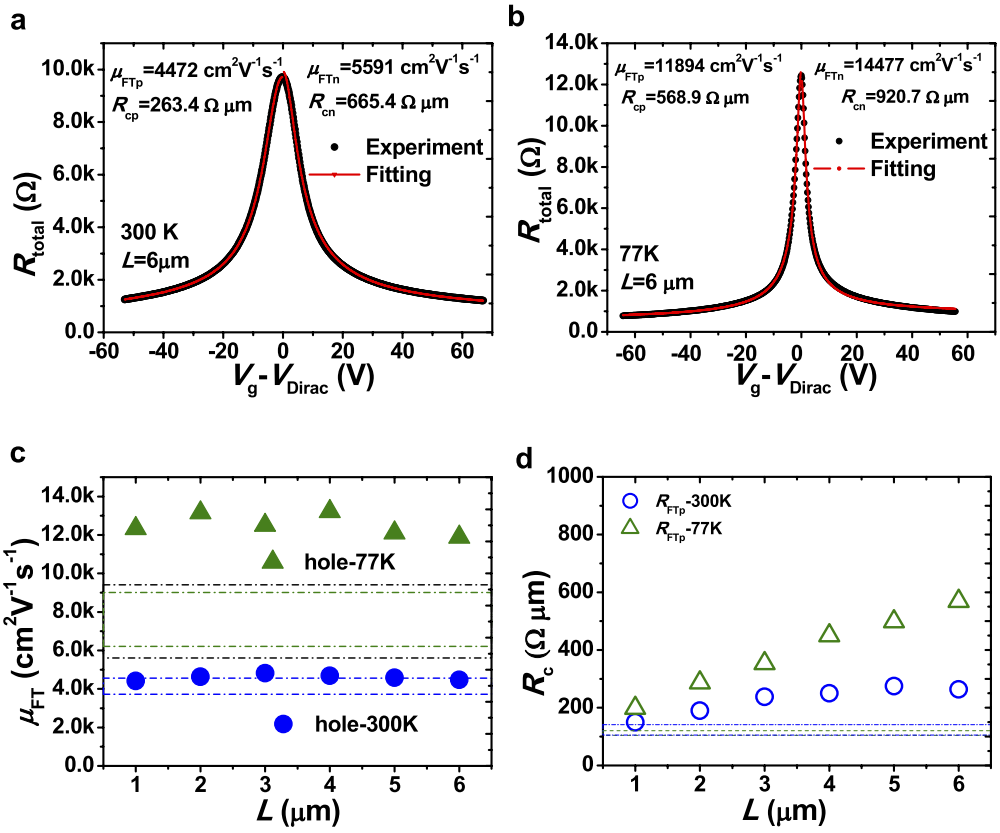

FIG. 3. The fitting model for mobility extraction. The experimental and fitted R_{total}-(V_g-V_{Dirac}) curves of the GFET with channel length of 6 um (a) at 300 K and (b) at 77 K. (c) The fitted hole mobility of the six GFETs at 300 K and 77 K. The blue (or olive) dotted rectangle represents the range of hole mobility at 300 K (77 K) given by TLM method at corresponding carrier density, where the black rectangle represents the range of hole mobility at 77 K by assuming n_0=0. (d) The fitted contact resistance of the six GFETs at 300 K and 77 K. The blue (or olive) dotted rectangle represents the range of contact resistance of p-branch (or n-branch) given by TLM method at corresponding gate voltage range.

the same way, the fitted mobility at 77 K are 11894 cm^2 V^{-1} s^{-1} for hole and 14477 cm^2 V^{-1} s^{-1} for electron, and the fitted R_c values are 569 Ω um in the p-branch and 921 Ω um in the n-branch.

The fitting method is quite popular as it provides a higher carrier mobility than DTM mobility and other parameters like contact resistance could also be obtained at the same time. It should be noted that the FTM takes the mobility and contact resistance as constant, while both of them depend on carrier density (gate voltage) in fact. Worst of all, the fitted mobility could be so high that it could match the value of mobility quite close to the Dirac point. In Fig. 3(c) and 3(d), hole mobility and contact resistance in the p-branch at two temperatures were plotted respectively, and as references the corresponding hole mobility and contact resistance at hole density ranging from 1.0×10^{12} cm^{-2} to 4.0×10^{12} cm^{-2} ($|V_g$-$V_{Dirac}|$ varies from 13.2 V to 53 V)[26] were given. At room temperature, all of the FTM mobility values locates at the upper side of the standard mobility range which correspond the carrier mobility at low density (1.0×10^{12} cm^{-2}). This is because that the FTM tends to focus the dots near Dirac point, and then is easy to overestimate the mobility. At 77 K, the FTM mobility values are even larger than the upper limits of standard mobility range, and then are corresponding to the values very close to the Dirac point. We also present the hole mobility arrange that assumes zero residual carrier density, which corresponding to the black line in Fig. 2(d). It should be noted that the mobility retrieved through FTM is almost a constant, independent of channel length, while the situation is different for contact resistance. Obviously, the FTM R_c increases with the channel length whatever at RT or 77 K, and the surplus over standard R_c range increases with increasing channel length. Therefore, for mobility fabrication of GFET with relative short channel is helpful to

TABLE I. Comparison of three mobility extracting methods based on field-effect measurements for graphene.

Method		TLM	DTM	TFM
Complexity of sample fabrication		High	Low	Low
Mobility	Accuracy	High	Underestimating	Overestimating
	Carrier density dependency	Yes	Yes	Constant
Contact resistance	Accuracy	High	Unable	Over-estimating
	Carrier density dependence	Yes	Unable	Constant

improve the accuracy of extracted carrier mobility and contact resistance through FTM, since both of the contact resistance and the ratio to the total channel resistance are relative high.

As a conclusion, we list the characteristics of the three methods, *i.e.* TLM, DTM and FTM, for mobility extraction based on field-effect measurements of graphene devices as shown in Table I. The TLM is the most accurate one at large carrier density since it eliminates the effect of contact resistance and offers carrier density dependent mobility and contact resistance as Hall measurements. Shortcoming of this method comes from its complexity, *i.e.* fabricating and measuring a group of devices with varying channel lengths and high uniformity. DTM is the easiest method and also provides carrier density dependent mobility. However, the method always underestimate carrier mobility due to the absolute neglect of the contact resistance. Accuracy of DTM method strongly depends on the ratio of contact resistance on the whole channel, and then GFET with long channel and good contact should be generally welcomed. FTM can provide more information than other two methods, such as carrier mobility, contact resistance and residual carrier density. However, the FTM actually assumes density independent mobility or contact resistance, and always overestimates the carrier mobility through compensating the total device resistance by higher contact resistance. Therefore, the FTM mobility should be carefully treated. Comparison of those three carrier mobility extraction methods illustrate that the TLM could not only be used to measure the contact resistance, but also be employed for carrier mobility extraction in GFET. And the TLM offers a much more accurate carrier density dependent carrier mobility of graphene than other two methods.

ACKNOWLEDGMENTS

This work was supported by the Ministry of Science and Technology of China (Grant Nos. 2011CB933001 and 2011CB933002), National Science Foundation of China (Grant Nos. 61322105, 61321001, 61390504 and 61427901).

[1] F. Schwierz, Nature Nanotechnology **5**, 487-496 (2010).
[2] P. Avouris and F. Xia, Mrs Bulletin **37**, 1225-1234 (2012).
[3] K. S. Novoselov, V. I. Falko, L. Colombo, P. R. Gellert, M. G. Schwab, and K. Kim, Nature **490**, 192-200 (2012).
[4] X. Li, W. Cai, J. An, S. Kim, J. Nah, D. Yang, R. Piner, A. Velamakanni, I. Jung, E. Tutuc, S. K. Banerjee, L. Colombo, and R. S. Ruoff, Science **324**, 1312-1314 (2009).
[5] K. S. Kim, Y. Zhao, H. Jang, S. Y. Lee, J. M. Kim, K. S. Kim, J.-H. Ahn, P. Kim, J.-Y. Choi, and B. H. Hong, Nature **457**, 706-710 (2009).
[6] L. Gao, W. Ren, H. Xu, L. Jin, Z. Wang, T. Ma, L.-P. Ma, Z. Zhang, Q. Fu, L.-M. Peng, X. Bao, and H.-M. Cheng, Nat Commun **3**, 699 (2012).
[7] S. Bae, H. Kim, Y. Lee, X. Xu, J.-S. Park, Y. Zheng, J. Balakrishnan, T. Lei, H. Ri Kim, Y. I. Song, Y.-J. Kim, K. S. Kim, B. Ozyilmaz, J.-H. Ahn, B. H. Hong, and S. Iijima, Nat Nano **5**, 574-578 (2010).
[8] W. Ren and H.-M. Cheng, Nat Nano **9**, 726-730 (2014).
[9] S. Park and R. S. Ruoff, Nat Nano **4**, 217-224 (2009).
[10] H. L. Xu, Z. Y. Zhang, R. B. Shi, H. G. Liu, Z. X. Wang, S. Wang, and L. M. Peng, Sci Rep **3**, 1207 (2013).
[11] L. Gao, G.-X. Ni, Y. Liu, B. Liu, A. H. Castro Neto, and K. P. Loh, Nature **505**, 190-194 (2014).
[12] X. Hong, A. Posadas, K. Zou, C. H. Ahn, and J. Zhu, Physical Review Letters **102**, 136808 (2009).
[13] Z. Liu, A. Bol, and W. Haensch, Nano Letters **11**, 523-528 (2010).
[14] S. Kim, J. Nah, I. Jo, D. Shahrjerdi, L. Colombo, Z. Yao, E. Tutuc, and S. K. Banerjee, Applied Physics Letters **94**, 062107 (2009).
[15] F. Xia, V. Perebeinos, Y.-m. Lin, Y. Wu, and P. Avouris, Nat Nano **6**, 179-184 (2011).

[16] D. K. Schroder, *Semiconductor and Material and Device Characterization*, Third Edition ed. (John Wiley & Sons, Inc, 2005).
[17] B. Huard, N. Stander, J. A. Sulpizio, and D. Goldhaber-Gordon, Phys. Rev. B **78**, 121402 (2008).
[18] G. Giovannetti, P. A. Khomyakov, G. Brocks, V. M. Karpan, J. van den Brink, and P. J. Kelly, Physical Review Letters **101**, 026803 (2008).
[19] D. S. Novikov, Physical Review B **76**, 245435 (2007).
[20] D. S. Novikov, Applied Physics Letters **91**, 102102 (2007).
[21] Y. B. Zhang, Y. W. Tan, H. L. Stormer, and P. Kim, Nature **438**, 201-204 (2005).
[22] W. Zhu, V. Perebeinos, M. Freitag, and P. Avouris, Physical Review B **80**, 235402 (2009).
[23] V. E. Dorgan, M. H. Bae, and E. Pop, Applied Physics Letters **97**, 082112 (2010).
[24] J.-H. Chen, C. Jang, S. Xiao, M. Ishigami, and M. S. Fuhrer, Nat Nano **3**, 206-209 (2008).
[25] L. Wang, I. Meric, P. Y. Huang, Q. Gao, Y. Gao, H. Tran, T. Taniguchi, K. Watanabe, L. M. Campos, D. A. Muller, J. Guo, P. Kim, J. Hone, K. L. Shepard, and C. R. Dean, Science **342**, 614-617 (2013).
[26] Actually, at 300 K, $|V_g\text{-}V_{Dirac}|$ is in the range from 13.2 to 50.2 V (corresponding to carrier density ranging from 1.0×10^{12} cm^{-2} to 3.797×10^{12} cm^{-2}) limited by the measured voltage range.